Z. angew. Math. Phys. 59 (2008) 124–144
0044-2275/08/010124-21
DOI 10.1007/s00033-007-6067-1


**Zeitschrift für angewandte Mathematik und Physik ZAMP**

# Channel flow of a Maxwell fluid with chemical reaction

T. Hayat and Z. Abbas[1]

**Abstract.** This work is concerned with the two-dimensional boundary layer flow of an upper-convected Maxwell (UCM) fluid in a channel with chemical reaction. The walls of the channel are porous. Employing similarity transformations the governing non-linear partial differential equations are reduced into non-linear ordinary differential equations. The resulting ordinary differential equations are solved analytically using homotopy analysis method (HAM). Expressions for series solutions are derived. The convergence of the obtained series solutions are shown explicitly. The effects of Reynold's number Re, Deborah number $De$, Schmidt number $Sc$ and chemical reaction parameter $\gamma$ on the velocity and the concentration fields are shown through graphs and discussed.

**Mathematics Subject Classification (2000).**

**Keywords.** Maxwell fluid, Boundary layer flow, Chemical reaction, HAM solution.

## 1. Introduction

For the last few decades the interest of scientists and engineers in viscoelastic flows has grown considerably due to their applications in biorheology, geophysics, chemical and petroleum industries. Due to complexity of fluids there is no single fluid model which exhibits all properties of viscoelastic fluids. Such fluids exhibit non-linear relationship between stress and the rate of strain and the corresponding flow equations in general are much more complicated, non-linear and higher order in comparison with that of the Newtonian fluids. There are very few cases in which the exact solutions of Navier-Stokes equations can be obtained. These are even rare if the constitutive relations for viscoelastic fluids are considered. Amongst the class of viscoelastic fluids the so-called second order fluid, first introduced by Rivlin and Ericksen [1] is that for which one can reasonably hope to obtain the analytic solutions. A series of interesting papers $[2-13]$ on the topic have appeared recently. But second order fluid model does not give reasonable results for flows of highly elastic fluids (polymer melts) that occur at high Deborah number [14]. For this reason the upper-convected Maxwell (UCM) fluid model is quite

[1] Corresponding author. Tel.: +92 51 2275341.

appropriate. Therefore such flow of UCM fluid is studied by Choi et al. [15]. Sadeghy et al. [16] analyzed the hydrodynamic flow of UCM fluid over a steadily moving plate. Hayat et al. [17] discussed the magnetohydrodynamic flow of UCM fluid over a porous stretching sheet.

All the above mentioned attempts involving UCM fluid describe the flow analysis without chemical reaction. Therefore in the present work we take important step towards obtaining the analytic solutions for porous channel flow with chemical reaction when the fluid belongs to the UCM category. We have developed HAM [18 − 35] solutions for velocity and concentration fields. The convergence of the obtained solution is explored. The influence of various interesting parameters on the velocity and concentration fields has been shown through graphs and discussed in great length.

## 2. Mathematical formulation

Let us consider the two-dimensional boundary layer flow of an incompressible Maxwell fluid in a porous channel with chemical reaction. Here $x$-axis is selected along the centerline of the channel, parallel to the channel surfaces and the $y$-axis transverse to these. The flow is symmetric about both the axes. The porous walls of the channel are at $y = H/2$ and $y = -H/2$ ($H$ is the channel width). The fluid injection or extraction takes place through the porous walls with velocity $V/2$. Here $V > 0$ corresponds to suction and $V < 0$ for injection. The concentration at $y = 0$ and $y = H/2$ are $C_w$ and $C_H$, respectively. Denoting $x$ and $y$ components of the velocity by $u$ and $v$ the equations of mass, momentum and the concentration field are

$$\frac{\partial u}{\partial x} + \frac{\partial v}{\partial y} = 0, \tag{1}$$

$$u\frac{\partial u}{\partial x} + v\frac{\partial u}{\partial y} + \lambda\left[u^2\frac{\partial^2 u}{\partial x^2} + v^2\frac{\partial^2 u}{\partial y^2} + 2uv\frac{\partial^2 u}{\partial x \partial y}\right] = \nu\frac{\partial^2 u}{\partial y^2}, \tag{2}$$

$$u\frac{\partial C}{\partial x} + v\frac{\partial C}{\partial y} = D\frac{\partial^2 C}{\partial y^2} - k_1 C. \tag{3}$$

In above equations $\nu$ is the kinematic viscosity, $\lambda$ is the relaxation time, $D$ is the mass diffusion, $C$ is the concentration field and $k_1$ denotes the reaction rate constant of the first-order homogeneous and irreversible reaction. Moreover, Eq. (2) has been derived in reference [16] and thus omitted here.

The symmetry about the $x$-axis and no-slip conditions at $y = H/2$ yield

$$\begin{aligned} &\frac{\partial u}{\partial y} = v = 0, \qquad C = C_w \quad \text{at} \quad y = 0, \\ &u = 0, \quad v = \frac{V}{2}, \qquad C = C_H \quad \text{at} \quad y = \frac{H}{2}. \end{aligned} \tag{4}$$

Defining the following non-dimensional transformations

$$x^* = \frac{x}{H}, \quad y^* = \frac{y}{H}, \quad u = -Vx^* f'(y^*), \quad v = Vf(y^*), \quad \phi = \frac{C - C_H}{C_w - C_H}, \tag{5}$$

Eq. (1) is satisfied identically and Eqs. (2)–(4) become

$$f''' + \mathrm{Re}(f'^2 - ff'') + De\left(2ff'f'' - f^2 f'''\right) = 0, \tag{6}$$

$$\phi'' - \mathrm{Re}Scf\phi' - Sc\gamma\phi = 0, \tag{7}$$

$$\begin{aligned} &f = 0, \quad f'' = 0, \quad \phi = 1, \quad \text{at} \quad y = 0, \\ &f = \frac{1}{2}, \quad f' = 0, \quad \phi = 0, \quad \text{at} \quad y = \frac{1}{2}. \end{aligned} \tag{8}$$

Here the Reynold's number (Re), Deborah number ($De$), the Schmidt number ($Sc$) and the chemical reaction parameter $\gamma$ are denoted by

$$\mathrm{Re} = HV/\nu, \qquad De = \lambda V^2/\nu, \qquad Sc = \frac{\nu}{D}, \qquad \gamma = \frac{H^2 k}{\nu}$$

and asterisks have been dropped for brevity. Further Re $> 0$ corresponds to suction and Re $< 0$ for injection. For the analytic solution of Eqs. (6)–(8) we employ HAM in the next section.

## 3. Analytical solution

In order to obtain the HAM solution we choose the initial guess and auxiliary linear operators in the following form

$$f_0(y) = y(\frac{3}{2} - 2y^2), \tag{9}$$

$$\phi_0(y) = 1 - 2y, \tag{10}$$

$$\mathcal{L}_1(f) = f''' \tag{11}$$

$$\mathcal{L}_2(f) = f'' \tag{12}$$

$$\mathcal{L}_1\left[C_1 + C_2 y + C_3 y^2\right] = 0, \tag{13}$$

$$\mathcal{L}_2\left[C_5 + C_4 y\right] = 0, \tag{14}$$

in which $C_i$, $(i = 1, 2....5)$ are arbitrary constants.

The problems at zeroth order satisfy

$$(1-p)\,\mathcal{L}_1\left[\widehat{f}(y,p) - f_0(y)\right] = p\hbar_1\mathcal{N}_1\left[\widehat{f}(y,p)\right], \tag{15}$$

$$(1-p)\,\mathcal{L}_2\left[\widehat{\phi}(y,p) - \phi_0(y)\right] = p\hbar_2\mathcal{N}_2\left[\widehat{f}(y,p), \widehat{\phi}(y,p)\right], \tag{16}$$

$$\widehat{f}(0,p)=0,\quad \widehat{f}''(0,p)=0,\quad \widehat{f}\left(\frac{1}{2},p\right)=\frac{1}{2},\quad \widehat{f}'\left(\frac{1}{2},p\right)=0, \tag{17}$$

$$\widehat{\phi}(0,p)=1,\quad \widehat{\phi}\left(\frac{1}{2},p\right)=0, \tag{18}$$

$$\begin{aligned}\mathcal{N}_1\left[\widehat{f}(y,p)\right] &= \frac{\partial^3\widehat{f}(y,p)}{\partial y^3}+\mathrm{Re}\left(\left(\frac{\partial\widehat{f}(y,p)}{\partial y}\right)^2-\widehat{f}(y,p)\frac{\partial^2\widehat{f}(y,p)}{\partial y^2}\right)\\ &+De\left\{2\widehat{f}(y,p)\frac{\partial\widehat{f}(y,p)}{\partial y}\frac{\partial^2\widehat{f}(y,p)}{\partial y^2}-\left(\widehat{f}(y,p)\right)^2\frac{\partial^3\widehat{f}(y,p)}{\partial y^3}\right\},\end{aligned} \tag{19}$$

$$\mathcal{N}_2\left[\widehat{f}(y,p),\widehat{\phi}(y,p)\right]=\frac{\partial^2\widehat{\phi}(\eta,p)}{\partial\eta^2}-Sc\gamma\widehat{\phi}(\eta,p)-\mathrm{Re}Sc\frac{\partial\widehat{\phi}(\eta,p)}{\partial\eta}\widehat{f}(\eta,p). \tag{20}$$

Here $p\in[0,1]$ is an embedding parameter and $\hbar_1$ and $h_2$ are the auxiliary nonzero parameters. For $p=0$ and $p=1$ we have

$$\begin{aligned}\widehat{f}(y,0)&=f_0(y), & \widehat{f}(y,1)&=f(y),\\ \widehat{\phi}(y,0)&=\phi_0(y), & \widehat{\phi}(y,1)&=\phi(y).\end{aligned} \tag{21}$$

Note that as $p$ increases from 0 to 1, $\widehat{f}(y,p)$ and $\widehat{\phi}(y,p)$ vary from $f_0(y)$ and $\phi_0(y)$ to $f(y)$ and $\phi(y)$ respectively. Due to Taylor's theorem and Eq. (21) one obtains

$$\widehat{f}(y,p)=f_0(y)+\sum_{m=1}^{\infty}f_m(y)p^m, \tag{22}$$

$$\widehat{\phi}(y,p)=\phi_0(y)+\sum_{m=1}^{\infty}\phi_m(y)p^m, \tag{23}$$

$$f_m(y)=\frac{1}{m!}\frac{\partial^m\widehat{f}(y,p)}{\partial p^m}\bigg|_{p=0},\quad \phi_m(y)=\frac{1}{m!}\frac{\partial^m\widehat{\phi}(y,p)}{\partial p^m}\bigg|_{p=0}. \tag{24}$$

Assume that $\hbar_1$ and $h_2$ are so properly chosen that the series (22) and (23) are convergent at $p=1$, we obtain from Eq. (21) that

$$f(y)=f_0(y)+\sum_{m=1}^{\infty}f_m(y),\qquad \phi(y)=\phi_0(y)+\sum_{m=1}^{\infty}\phi_m(y). \tag{25}$$

In order to get the mth-order deformation equation, we first differentiate Eqs. (15) and (16) $m$ times with respect to $p$ at $p=0$ and then divide by $m!$

$$\mathcal{L}_1\left[f_m(y)-\chi_m f_{m-1}(y)\right]=\hbar_1\mathcal{R}_{1m}(y), \tag{26}$$

$$\mathcal{L}_2\left[\phi_m(y)-\chi_m\phi_{m-1}(y)\right]=\hbar_2\mathcal{R}_{2m}(y). \tag{27}$$

The boundary conditions are

$$f_m(0) = f''_m(0) = f_m\left(\frac{1}{2}\right) = f'_m\left(\frac{1}{2}\right) = 0,$$
$$\phi_m(0) = \phi_m\left(\frac{1}{2}\right) = 0, \tag{28}$$

where

$$\mathcal{R}_{1m}(y) = f'''_{m-1} + \sum_{k=0}^{m-1}\left[\mathrm{Re}\left(f'_{m-1-k}f'_k - f_{m-1-k}f''_k\right) + Def_{m-1-k}\sum_{l=0}^{k}\left\{2f'_{k-l}f''_l - f_{k-l}f'''_l\right\}\right], \tag{29}$$

$$\mathcal{R}_{2m}(y) = \phi''_{m-1} - Sc\gamma\phi_{m-1} - \mathrm{Re}Sc\sum_{k=0}^{m-1}\phi'_{m-1-k}f_k, \tag{30}$$

$$\chi_m = \left|\begin{array}{ll} 0, & m \leq 1, \\ 1, & m > 1. \end{array}\right. \tag{31}$$

It should be noted that in Eq. (28), there are four boundary conditions for $f_m$. However, we use the third-order linear operator defined by Eq. (11) to get the reasonable $\hbar$-curve. Here we use such a solution expression that one of the boundary conditions must be automatically satisfied. The solution of problem consisting of Eqs. (26)–(28) up to first few order of approximations can be obtained using symbolic software MATHEMATICA. It is found that $f_m(y)$ and $\phi_m(y)$ can be expressed by

$$f_m(y) = \sum_{n=0}^{6m+3} a_{m,n}y^n, \qquad m \geq 0, \tag{32}$$

$$\phi_m(y) = \sum_{n=0}^{6m+1} b_{m,n}y^n, \qquad m \geq 0, \tag{33}$$

where $a_{m,n}$ and $b_{m,n}$ are the coefficients. Invoking Eqs. (32) and (33) into Eqs. (26) and (27) we have for $m \geq 1$, $0 \leq n \leq 6m+3$ and $m \geq 1$, $0 \leq n \leq 6m+1$ as

$$a_{m,1} = \chi_m\chi_{6m-2}a_{m-1,1} + \sum_{n=0}^{6m+3}\frac{\Delta_{m,n}}{(n+1)(n+2)2^{n+2}},$$

$$a_{m,2} = \chi_m\chi_{6m-4}a_{m-1,2} - \sum_{n=0}^{6m+3}\frac{\Delta_{m,n}}{(n+1)(n+2)2^{n+1}},$$

$$a_{m,n} = \chi_m\chi_{6m-1-n}a_{m-1,n} + \sum_{n=0}^{6m+3}\frac{\Delta_{m,n-3}}{n(n-1)(n-2)}, \quad n \geq 3,$$

$$b_{m,1} = \chi_m \chi_{6m-4} b_{m-1,1} - \sum_{n=0}^{6m+1} \frac{\Gamma_{m,n}}{(n+1)(n+2)2^{n+1}},$$

$$b_{m,2} = \chi_m \chi_{6m-5} b_{m-1,2} + \sum_{n=0}^{6m+1} \frac{\Gamma_{m,n}}{(n+1)(n+2)},$$

$$b_{m,n} = \chi_m \chi_{6m-3-n} b_{m-1,n} + \sum_{n=0}^{6m+1} \frac{\Gamma_{m,n-2}}{n(n-1)}, \quad n \geq 2,$$

$$\Delta_{m,n} = \hbar_1 \left[ \chi_{6m-1-n} d_{m-1,n} + \chi_{6m-n+2} \mathrm{Re} \left( \alpha_{m,n} - \beta_{m,n} \right) + De \left( 2\gamma_{m,n} - \delta_{m,n} \right) \right], \tag{34}$$

$$\Gamma_{m,n} = \hbar_2 \left[ \chi_{6m-3-n} (g_{m-1,n} - Sc\gamma b_{m-1,n}) - \chi_{6m-n} \mathrm{Re} Sc \delta 1_{m,n} \right]. \tag{35}$$

The coefficients $\alpha_{m,n}$, $\beta_{m,n}$, $\gamma_{m,n}$, $\delta_{m,n}$ and $\delta 1_{m,n}$, when $m \geq 1$, $0 \leq n \leq 6m+3$ and $0 \leq n \leq 6m+1$ are

$$\alpha_{m,n} = \sum_{k=0}^{m-1} \sum_{j=\max\{0,n-6m+6k+3\}}^{\min\{n,6k+3\}} c_{k,j} c_{m-1-k,n-j},$$

$$\beta_{m,n} = \sum_{k=0}^{m-1} \sum_{j=\max\{0,n-6m+6k+3\}}^{\min\{n,6k+3\}} d_{k,j} a_{m-1-k,n-j},$$

$$\gamma_{m,n} = \sum_{k=0}^{m-1} \sum_{l=0}^{k} \sum_{q=\max\{0,n-6m+6k+3\}}^{\min\{n,6k+6\}} \sum_{j=\max\{0,q-6k+6l-3\}}^{\min\{r,6l+3\}} d_{k,j} c_{k-l,q-j} a_{m-1-k,n-q},$$

$$\delta_{m,n} = \sum_{k=0}^{m-1} \sum_{l=0}^{k} \sum_{q=\max\{0,n-6m+6k+3\}}^{\min\{n,6k+6\}} \sum_{j=\max\{0,q-6k+6l-3\}}^{\min\{r,6l+3\}} e_{k,j} a_{k-l,q-j} a_{m-1-k,n-q},$$

$$\delta 1_{m,n} = \sum_{k=0}^{m-1} \sum_{j=\max\{0,n-6m+6k+5\}}^{\min\{n,6k+3\}} a_{k,j} f_{m-1-k,n-j},$$

where

$$\begin{aligned} c_{m,n} &= (n+1)\, a_{m,n+1}, \\ d_{m,n} &= (n+1)\, c_{m,n+1}, \\ e_{m,n} &= (n+1)\, d_{m,n+1}, \end{aligned} \tag{36}$$

$$\begin{aligned} f_{m,n} &= (n+1)\, b_{m,n+1}, \\ g_{m,n} &= (n+1)\, f_{m,n+1} \end{aligned} \tag{37}$$

and the detailed procedure for the derivation of the above relations is given in reference [20]. Due to above recurrence formulae, we can calculate all coefficients $a_{m,n}$ and $b_{m,n}$ using only the first few

$$a_{0,0} = a_{0,2} = 0, \quad a_{0,1} = \frac{3}{2}, \quad a_{0,3} = -2, \quad b_{0,0} = 1, \quad b_{0,1} = -2 \tag{38}$$

given by the initial guess approximation in Eqs. (9) and (10).

Therefore, we obtain an explicit analytic solution of the following form

$$f(y) = \sum_{m=0}^{\infty} f_m(y) = \lim_{M\to\infty} \left[ \sum_{n=1}^{6M+3} \left( \sum_{m=n-1}^{6M+2} a_{m,n} y^n \right) \right], \tag{39}$$

$$\phi(y) = \sum_{m=0}^{\infty} \phi_m(y) = \lim_{M\to\infty} \left[ \sum_{n=1}^{6M+1} \left( \sum_{m=n-1}^{6M} b_{m,n} y^n \right) \right]. \tag{40}$$

## 4. Convergence of the HAM solution

The analytic solution of the considered problem is obtained and given in Eqs. (39) and (40). One needs to guarantee the convergence of the series (39) and (40). Liao [18] pointed out that the convergence and rate of approximation for the HAM solution strongly depends on the values of auxiliary parameters $\hbar_1$ and $\hbar_2$. One can check the range of the admissible values of $\hbar_1$ and $h_2$ by drawing the so-called $\hbar$-curves. For the present analysis the $\hbar$-curves are plotted for two different orders of approximations in Figs. 1 and 2. It is evident from these Figs. that the admissible range for the values of $\hbar_1$ and $h_2$ is $-1.8 \le \hbar_{1,2} \le -0.2$. It is also noted that the interval for the admissible values of $\hbar_1$ and $\hbar_2$ increases by increasing the order of approximation. It is found that the series (39) and (40) converge in the whole region of $y$ when $\hbar_{1,2} = -1$.

## 5. Results and discussion

In this section the results are obtained just to see the variations of $De$, Re, $Sc$ and $\gamma$ on the velocity components $f$ and $f'$ and concentration field $\phi$ for both suction and injection. Subsections 5.1 and 5.2 describe the respective results of Newtonian ($De = 0$) and viscoelastic fluids ($De \neq 0$). For this purpose Figs. 3–24 have been plotted. Note that for suction case Re $> 0$ and Re $< 0$ corresponds to the injection case.

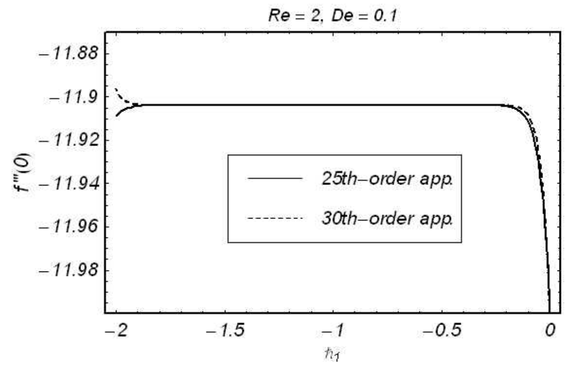


Figure 1. $\hbar_1$-curve for the 25th and 30th-order of approximations.

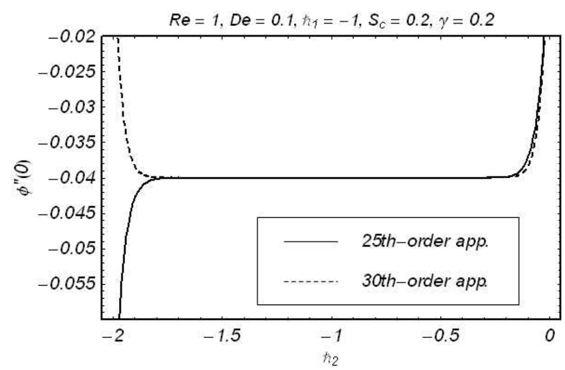


Figure 2. $\hbar_2$-curve for the 25th and 30th-order of approximations.

### 5.1. Newtonian fluid $(De = 0)$

Figs. 3–8 are plotted in order to see the effects of Reynolds number Re, the Schmidt number $Sc$ and the chemical reaction parameter $\gamma$ on the velocity components $f$ and $f'$ and the concentration field $\phi$ for a Newtonian fluid with suction and injection.

Figs. 3 and 4 show the variation of Re on $f$ and $f'$. It is quite apparent from these figures. that for large Re $(> 0)$ $f$ decreases and $f'$ initially decreases. But $f'$ increases by increasing suction Reynolds number after $y = 0.25$. Fig. 4 elucidates that the behavior for Re $(< 0)$ is quite opposite to that given in Fig. 3. But the change in $f$ (Fig. 4) is noted very small.

Figs. 5–8 have been prepared for the variations of Re, $Sc$ and $\gamma$ on $\phi$ for both suction and injection. The effects of Re $(> 0)$ on $\phi$ are plotted in Fig. 5. It is evident that $\phi$ increases by increasing suction Reynolds number Re $(> 0)$ whereas

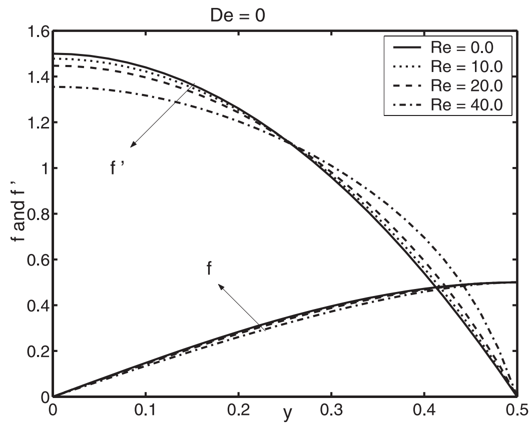


Figure 3. Effects of suction $Re$ on $f$ and $f'$at $\hbar_1 = -1$.

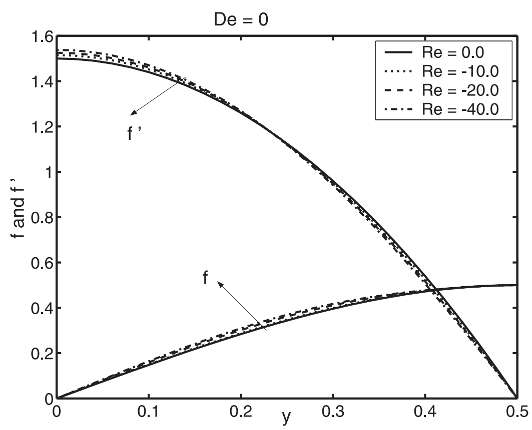


Figure 4. Effects of injection $Re$ on $f$ and $f'$at $\hbar_1 = -1$.

it decreases in injection case (Fig. 6). Fig. 7 gives that $\phi$ increases by increasing the suction Reynolds number Re $(> 0)$ and it decreases in the case of injection Re $(< 0)$. Moreover it is noted from Fig. 8 that $\phi$ is an increasing function of $\gamma$ in both suction and injection cases. But it is worth mentioning that the magnitude of $\phi$ in suction case is greater when compared with that of injection and this change occurs at very large values of $\gamma$.

### 5.2. Viscoelastic (non-Newtonian) fluid $(De \neq 0)$

#### 5.2.1. Suction flow $(\mathrm{Re} \geq 0,\ De > 0)$

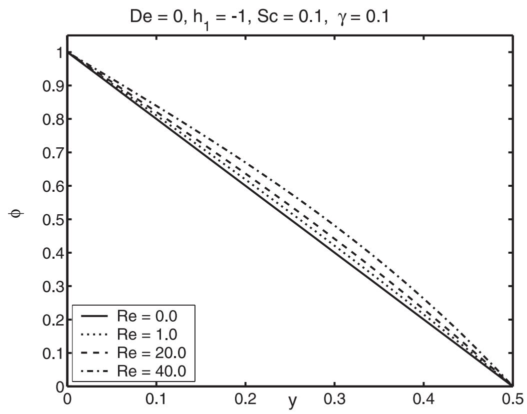


Figure 5. Effects of suction $Re$ on $\phi$ at $\hbar_2 = -1$.

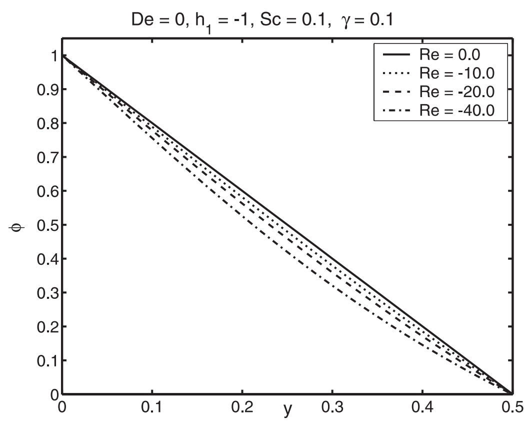


Figure 6. Effects of injection $Re$ on $\phi$ at $\hbar_2 = -1$.

Here Figs. 9–18 depict the variations of Re, $De$, $Sc$ and $\gamma$ on $f$, $f'$ and $\phi$.

From Figs. 9–11, we can see the effects of Re and $De$ on $f$ and $f'$. Fig. 9 illustrates the variation of Re ($> 0$) on $f$ and $f'$ by keeping $De$ fixed. It is interesting to note that here results of $f$ and $f'$ are almost similar to that of Newtonian fluid for small Deborah number $De = 0.1$. Fig. 10 has been prepared for the variation of $De$ on $f$ and $f'$ when $\mathrm{Re} = 0$. Here although $f$ increases for large $De$ but this increment is almost very small. However $f'$ increases initially and decreases after $y = 0.3$. The variation of $De$ on $f$ and $f'$ for $\mathrm{Re} = 0$ is shown in Fig. 11. It is worthnoting that results here are quite opposite in comparison to Fig. 10. Further, the more flattening of velocity occurs by increasing $De$ and large Re.

In order to see the effects of Re, $De$, $Sc$ and $\gamma$ on $\phi$, we depict Figs. 12–18.

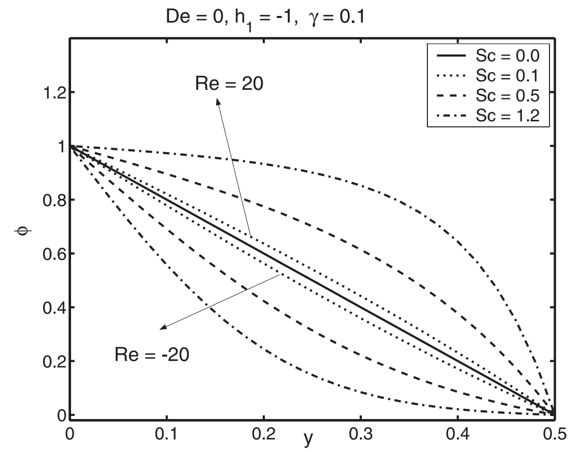


Figure 7. Effects of $Sc$ on $\phi$ at $\hbar_2 = -1$.

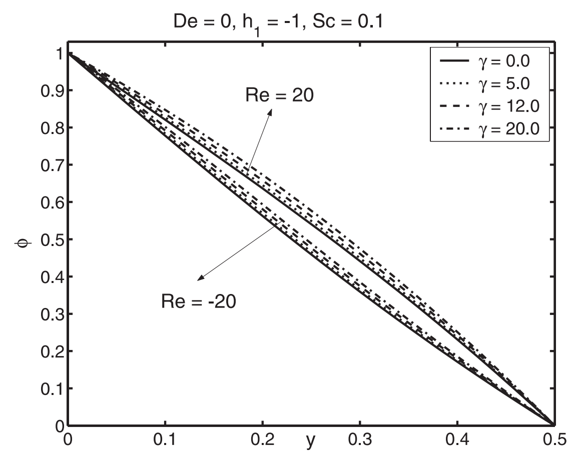


Figure 8. Effects of $\gamma$ on $\phi$ at $\hbar_2 = -1$.

| $\eta$ | $De$ | $f$ | $f'$ | $\phi$ |
|---|---|---|---|---|
| 0.1 | 0.0 | 0.134246 | 1.317430 | 1.199770 |
| | 0.5 | 0.133665 | 1.311560 | 1.197280 |
| | 1.0 | 0.133168 | 1.306340 | 1.196370 |
| | 1.5 | 0.132857 | 1.302650 | 1.198260 |
| | 2.0 | 0.132828 | 1.301220 | 1.204460 |
| | 5.0 | 0.096590 | 0.942991 | 1.422180 |

Table 1. Variations of physical parameters on $f$, $f'$ and $\phi$ at $\mathrm{Re} = 40$ in case of suction.

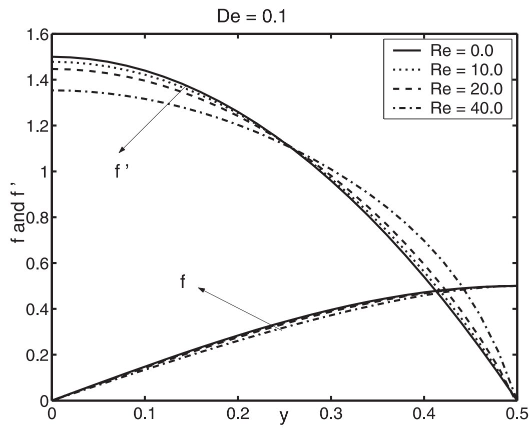


Figure 9. Effects of suction $Re$ on $f$ and $f'$at $\hbar_1 = -1$.

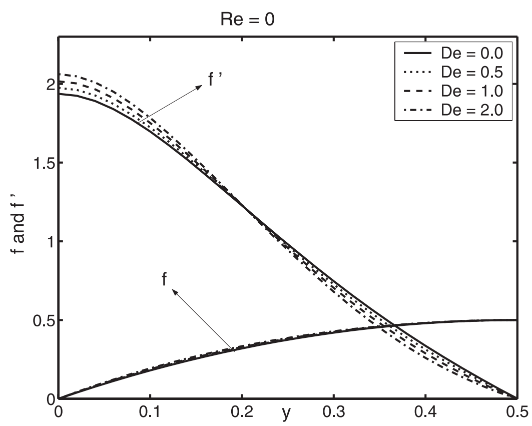


Figure 10. Effects of $De$ on $f$ and $f'$at $\hbar_1 = -1$.

Fig. 12 shows that $\phi$ is an increasing function of $De \neq 0$ when suction Reynolds number Re is increased. Figs. 13 and 14 indicate the behavior of $De$ on $\phi$ for fixed Re. The concentration field $\phi$ is a decreasing function of $De$ for Re (fixed). But the behavior of $De$ on $\phi$ is larger for small Re (approximately equal to zero) when compared with high Re. Fig. 15 shows that $\phi$ increases for small Re and large values of $Sc$. Fig. 16 depicts that $\phi$ increases for small $Sc$ and large Re. The comparison of these two figures indicates that the variation in Fig. 16 is more. Figs. 17 and 18 further elucidate the influence of $\gamma$ on $\phi$. These figures show that $\phi$ is an increasing function of $\gamma$. For small Re the change in $\phi$ is greater at high Deborah number $De = 1$. For Re = 20 and $De = 0.1$ the change is small (Fig.18).

Table 1 shows the valid range of the physical parameters $De$ and suction/injec-

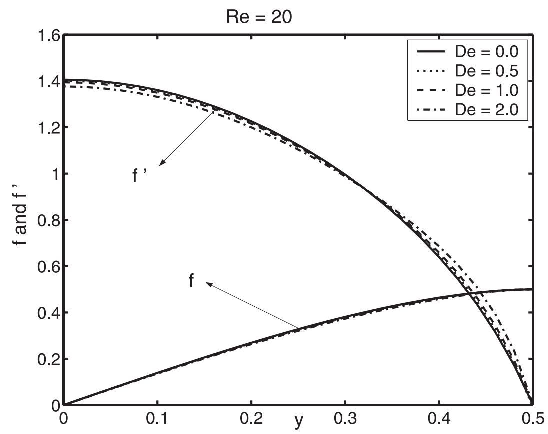


Figure 11. Effects of $De$ on $f$ and $f'$at $\hbar_1 = -1$.

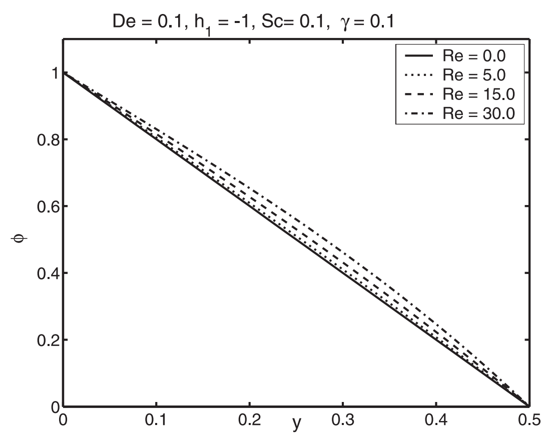


Figure 12. Effects of suction $Re$ on $\phi$ at $\hbar_2 = -1$.

tion Reynold's number Re on the velocity profiles $f$ and $f'$ and the concentration field $\phi$ in the suction case. It is observed that for $0 \leq De \leq 5$ and $0 \leq \text{Re} \leq 40$ the convergent solution exists.

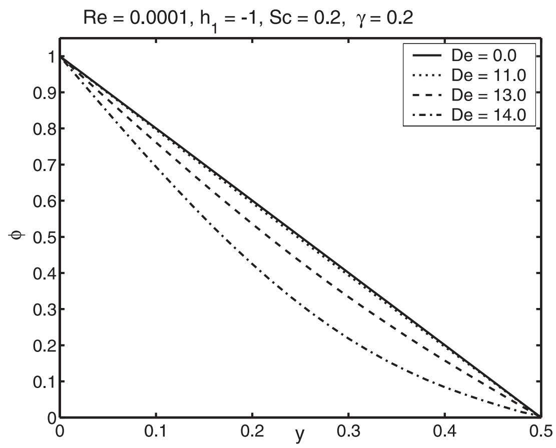


Figure 13. Effects of $De$ on $\phi$ at $\hbar_2 = -1$.

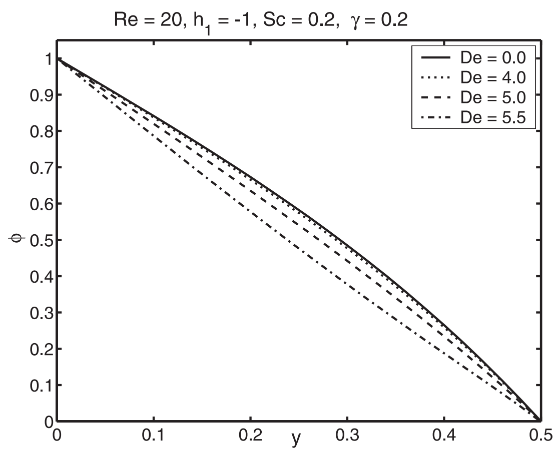


Figure 14. Effects of $De$ on $\phi$ at $\hbar_2 = -1$.

**5.2.2 Injection flow** (Re $< 0$, $De < 0$)

Figs. 19–24 are drawn in order to see the effects of Re, $De$, $Sc$ and $\gamma$ on $f$, $f'$ and $\phi$ for a viscoelastic fluid ($De < 0$) in the case of injection Re ($< 0$).

Figs. 19 and 20 present the effects of Re and $De$ on $f$ and $f'$. Fig. 19 shows that $f$ and $f'$ are increased by increasing the injection Reynolds number Re. Here $f'$ initially increases and then decreases after $y = 0.3$. From Fig. 20 we can see that $f$ and $f'$ decrease when $De$ increases but $f'$ increases much after $y = 0.3$. Fig. 21 illustrates the variation of Re ($< 0$) on $\phi$. It is noted that $\phi$ decreases by increasing injection Reynolds number Re. Fig. 22 gives the effects of $De$ on $\phi$. Obviously $\phi$ is an increasing function of $De$. Further the variations of $Sc$ and

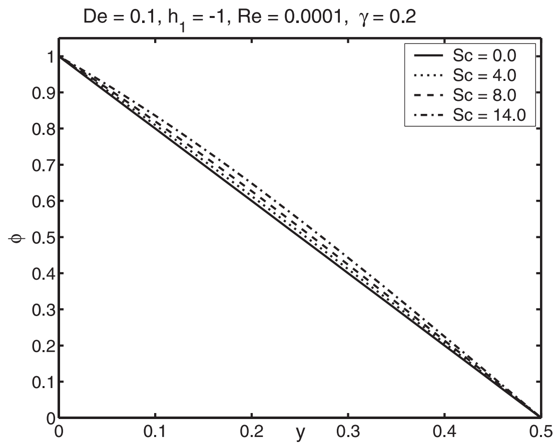


Figure 15. Effects of $Sc$ on $\phi$ at $\hbar_2 = -1$.

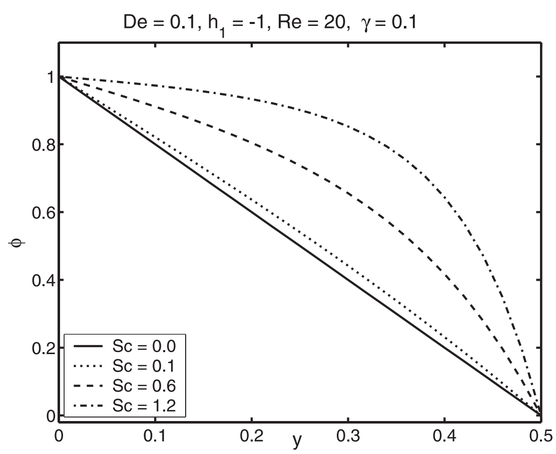


Figure 16. Effects of $Sc$ on $\phi$ at $\hbar_2 = -1$.

$\gamma$ on $\phi$ can be seen through Figs. 23 and 24. Fig. 23 elucidates that $\phi$ decreases and increases in Fig. 24 by increasing $Sc$ and $\gamma$ respectively. But from Fig. 24 it is noted that the change in $\phi$ occurs at very high $\gamma$.

Table 2 shows the valid range of the physical parameters $De$, suction/injection Reynold's number Re, $Sc$ and $\gamma$ on the velocity profiles $f$ and $f'$ and the concentration field $\phi$ in the injection case, respectively. It is noted that for $0 \leq De \leq -5$, $0 \leq \text{Re} \leq -40$, $0 \leq Sc \leq 1$ and $0 \leq \gamma \leq 20$ the convergent solution exists.

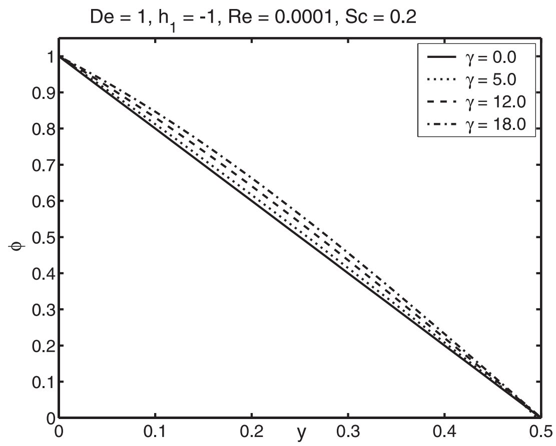


Figure 17. Effects of $\gamma$ on $\phi$ at $\hbar_2 = -1$.

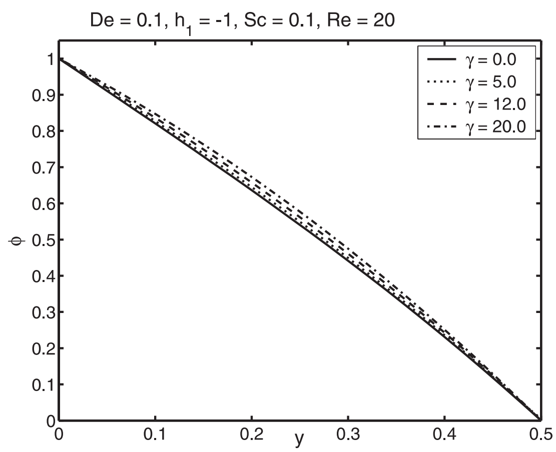


Figure 18. Effects of $\gamma$ on $\phi$ at $\hbar_2 = -1$.

## 6. Concluding remarks

The present study describes the boundary layer flow of Maxwell fluid with chemical reaction in a porous channel. The governing non-linear equations are solved analytically using HAM. Graphical results of velocity and concentration fields are plotted and discussed. The following observations have been made.

- For suction and injection, the influence of Re on the velocity and concentration fields is opposite when $De = 0$.
- The velocity has opposite behavior in viscoelastic fluid ($De \neq 0$) by increasing Reynolds number Re but has the same behavior for the variation of

| $\eta$ | $De$ | $f$ | $f'$ | $\phi$ |
|---|---|---|---|---|
| 0.1 | 0.0 | 0.151645 | 1.471380 | 0.775865 |
| | −0.5 | 0.151608 | 1.471420 | 0.774516 |
| | −1.0 | 0.151538 | 1.471140 | 0.772980 |
| | −1.5 | 0.151362 | 1.469870 | 0.771257 |
| | −2.0 | 0.150994 | 1.466370 | 0.769325 |
| | −5.0 | 0.134322 | 1.321900 | 0.751991 |

Table 2. Variations of physical parameters on $f$, $f'$ and $\phi$ at $\mathrm{Re} = -40$, $Sc = 1$ and $\gamma = 20$ in case of injection.

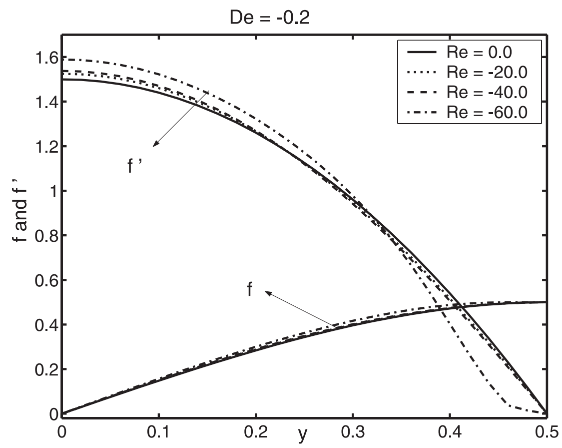


Figure 19. Effects of suction $Re$ on $f$ and $f'$at $\hbar_1 = -1$.

$De$.

- For suction and injection, the effects of Re on the concentration field are opposite $De \neq 0$.
- For $De \neq 0$, the concentration field has opposite behavior in suction and injection.
- The concentration field has opposite results for $Sc$ and same for $\gamma$ in suction and injection when $De \neq 0$.
- All results given in Figs. 3–24 are convergent at $\hbar_1 = \hbar_2 = -1$.
- To the best of our knowledge the present solutions are not reported in the literature. Even such solutions are not yet available for a Newtonian fluid. The results corresponding to Newtonian fluid can be obtained by putting $De = 0$.

## Acknowledgements

We are thankful to the referees for their helpful suggestions. The financial support from Higher Education Commission (HEC) is also gratefully acknowledged.

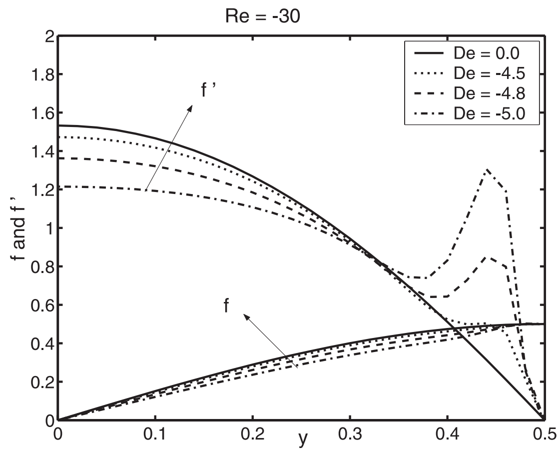


Figure 20. Effects of $De$ on $f$ and $f'$at $\hbar_1 = -1$.

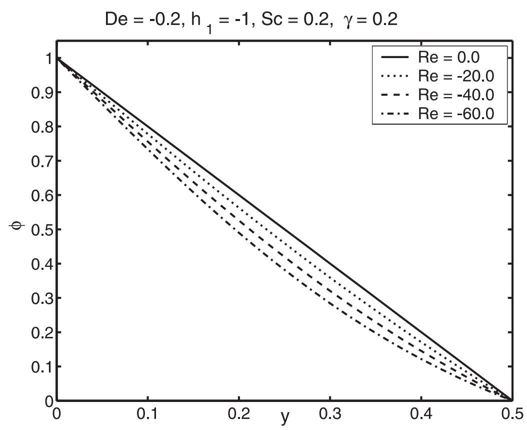


Figure 21. Effects of $De$ on $f$ and $f'$at $\hbar_1 = -1$.

## References


[1] R. S. Rivlin and J. L. Ericksen, Stress deformation relation for isotropic materials, *J. Rat. Mech. Anal.* **4** (1955), 323–425.

[2] T. Hayat, M. Khan, A. M. Siddiqui and S. Asghar, Transient flows of a second grade fluid, *Int. J. Non-Linear Mech.* **39** (2004), 1621–1633.

[3] T. Hayat, Y. Wang and K. Hutter, Hall effects on the unsteady hydromagnetic oscillatory flow of a second grade fluid, *Int. J. Non-Linear Mech.* **39** (2004), 1027–1037.

[4] K. R. Rajagopal, A note on unsteady unidirectional flows of a non-Newtonian fluid. *Int. J. Non-Linear Mech.* **17** (1982), 369–373.

[5] K. R. Rajagopal, On the creeping flow of the second grade fluid, *J. Non-Newtonian Fluid Mech.* **15** (1984), 239–246.

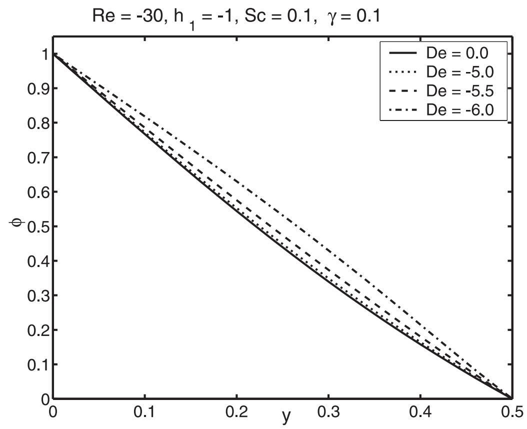


Figure 22. Effects of suction $Re$ on $\phi$ at $\hbar_2 = -1$.

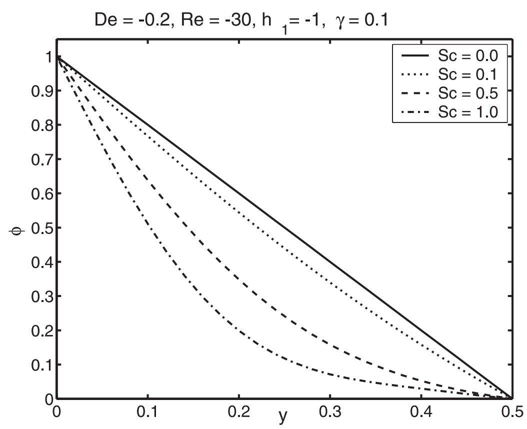


Figure 23. Effects of $De$ on $\phi$ at $\hbar_2 = -1$.

[6] C. Fetecau and J. Zierep, On a class of exact solutions of the equations of motion of a second grade fluid, *Acta Mech.* **150** (2001), 135–138.

[7] C. Fetecau, C. Fetecau and J. Zierep, Decay of a potential vortex and propagation of a heat wave in a second grade fluid, *Int. J. Non-Linear Mech.* **37** (2002), 1051–1056.

[8] C. Fetecau and C. Fetecau, On some axial Couette flows of non-Newtonian fluids, *Z. Angew. Math. Phys. (ZAMP)* **56** (2005), 1098–1106.

[9] C. Fetecau and C. Fetecau, Starting solutions for some unsteady unidirectional flows of a second grade fluid, *Int. J. Eng. Sci.* **43** (2005), 781–789.

[10] S. Asghar, T. Hayat and A. M. Siddiqui, Moving boundary in a non-Newtonian fluid, *Int. J. Non-Linear Mech.* **37** (2002), 75–80.

[11] W. C. Tan and T. Masuoka, Stokes first poroblem for second grade fluid in a porous half space, *Int. J. Non-Linear Mech.* **40** (2005), 515–522.

[12] K. Sadeghy and M. Sharifi, Local similarity solution for the flow of a "second-grade" viscoelastic fluid above a moving plate, *Int. J. Non-Linear Mech.* **39** (2004), 1265–1273.

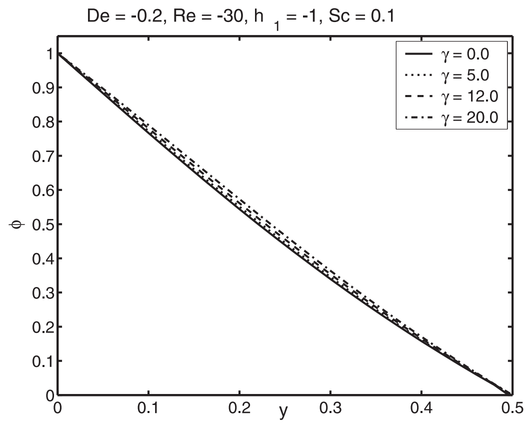


Figure 24. Effects of $De$ on $\phi$ at $\hbar_2 = -1$.


[13] K. Vajravelu and T. Roper, Flow and heat transfer in a second grade fluid over a stretching sheet, *Int. J. Non-Linear Mech.* **34** (1999), 1031–1036.

[14] R. B. Bird, R. C. Armstrong and O. Hassager, *Dynamics of Polymeric Liquids, vols. I and II*, Wiley, New York 1987.

[15] J. J. Choi, Z. Rusak and J. A. Tichy, Maxwell fluid suction flow in a channel, *J. Non-Newtonian Fluid Mech.* **85** (1999), 165–187.

[16] K. Sadeghy, A. H. Najafi and M. Saffaripour, Sakiadis flow of an upper-convected Maxwell fluid, *Int. J. Non-Linear Mech.* **40** (2005) 1220–1228.

[17] T. Hayat, Z. Abbas and M. Sajid, Series solution for the upper-convected Maxwell fluid over a porous stretching plate, *Phys. Letters A.* **358** (2006), 396–403.

[18] S. J. Liao, Beyond perturbation: introduction to homotopy analysis method, Chapman & Hall/CRC Press, Boca Raton 2003.

[19] S. J. Liao, On the homotopy analysis method for nonlinear problems, *Appl. Math. Comput.* **147** (2004) 499–513.

[20] S. J. Liao, A uniformly valid analytic solution of 2D viscous flow past a semi-infinite flat plate, *J. Fluid Mech.* **385** (1999), 101–128.

[21] S. J. Liao and A. Campo, Analytic solutions of the temperature distribution in Blasius viscous flow problems, *J. Fluid Mech.* **453** (2002), 411–425.

[22] S. J. Liao, On the analytic solution of magnetohydrodynamic flows of non-Newtonian fluids over a stretching sheet, *J. Fluid Mech.* **488** (2003), 189–212.

[23] S. J. Liao and K. F. Cheung, Homotopy analysis of nonlinear progressive waves in deep water, *J. Eng. Math.* **45** (2003), 105–116.

[24] M. Ayub, A. Rasheed and T. Hayat, Exact flow of a third grade fluid past a porous plate using homotopy analysis method, *Int. J. Eng. Sci.* **41** (2003), 2091–2103.

[25] T. Hayat, M. Khan and M. Ayub, On the explicit analytic solutions of an Oldroyd 6-constant fluid, *Int. J. Eng. Sci.* **42** (2004), 123–135.

[26] T. Hayat, M. Khan and M. Ayub, Couette and Poiseuille flows of an Oldroyd 6-constant fluid with magnetic field, *J. Math. Anal. & Appl.* **298** (2004), 225–244.

[27] T. Hayat, M. Khan and S. Asghar, Homotopy analysis of MHD flows of an Oldroyd 8-constant fluid, *Acta Mech.* **168** (2004), 213–232.

[28] C. Yang and S. J. Liao, On the explicit purely analytic solution of Von Karman swirling viscous flow, *Comm. Non-linear Sci. Numer. Simm.* **11** (2006), 83–93.

[29] S. J. Liao, A new branch of solutions of boundary-layer flows over an impermeable stretched plate, *Int. J. Heat and Mass Transfer* **48** (2005), 2529–2539.
[30] S. J. Liao, An analytic solution of unsteady boundary-layer flows caused by an impulsively stretching plate, *Comm. Non-linear Sci. Numer. Simm.* **11** (2006), 326–339.
[31] T. Hayat and M. Khan, Homotopy solution for a generalized second grade fluid past a porous plate, *Non-Linear Dynamics* **42** (2005), 395–405.
[32] W. Wu and S. J. Liao, Solving solitary waves with discontinuity by means of the homotopy analysis method, *Chaos, Solitons & Fractals* **26** (2005), 177–185.
[33] Y. Y. Wu, C. Wang and S. J. Liao, Solving the one loop solution of the Vakhnenko equation by means of the homotopy analysis method, *Chaos, Solitons & Fractals.* **23** (2005), 1733–1740.
[34] T. Hayat, M. Khan and S. Asghar, Magnetohydrodynamic flow of an Oldroyd 6-constant fluid, *Appl. Math. Comput.* **155** (2004), 417–425.
[35] M. Sajid, T. Hayat and S. Asghar, On the analytic solution of the steady flow of a fourth grade fluid, *Phys. Letters A.* **355** (2006), 18–26.

T. Hayat and Z. Abbas
Department of Mathematics
Quaid-I-Azam University 45320
Islamabad 44000
Pakistan
e-mail: za_qau@yahoo.com

(Received: June 26, 2006; revised: January 11, 2007)

Published Online First: June 12, 2007